Reply to "Comment on 'Diamagnetism and Cooper pairing above T_c in cuprates' "

Lu Li,[1,2] Yayu Wang,[1,3] and N. P. Ong[1]
[1]*Department of Physics, Princeton University, Princeton, New Jersey 08544, USA*
[2]*Department of Physics, University of Michigan, Ann Arbor, Michigan 48109, USA*
[3]*Department of Physics, Tsinghua University, Beijing, China*
(Received 17 August 2012; published 19 February 2013)

We analyze recent torque measurements of the magnetization M_d vs magnetic field H in optimally doped $YBa_2Cu_3O_{7-y}$ (OPT YBCO) to argue against a recent proposal by R. I. Rey *et al.* [Phys. Rev. B **87**, 056501 (2013)] that the magnetization results above T_c are consistent with Gaussian fluctuations. We find that despite its strong interlayer coupling, OPT YBCO displays an anomalous nonmonotonic dependence of M_d on H which represents direct evidence for the locking of the pair wave function phase θ_n at T_c and the subsequent unlocking by a relatively weak H. These unusual features characterize the unusual nature of the transition to the Meissner state in cuprate superconductors. They are absent in low-T_c superconductors to our knowledge. We also stress the importance of the vortex liquid state, as well as the profiles of the melting field $H_m(T)$ and the upper critical field curve $H_{c2}(T)$ in the T-H plane. Contrary to the claims of Rey *et al.*, we show that the curves of the magnetization and the Nernst signal illustrate the inaccessibility of the H_{c2} line near T_c. The prediction of the H_{c2} line by Rey *et al.* is shown to be invalid in OPT YBCO.

DOI: 10.1103/PhysRevB.87.056502 PACS number(s): 74.25.Dw, 74.25.Ha, 74.72.−h

I. INTRODUCTION

In the mean-field Gaussian treatment of fluctuations (valid in low-T_c superconductors), the pair wave function amplitude $|\Psi|$ vanishes at the critical temperature T_c. Above T_c, amplitude fluctuations about the equilibrium point $|\Psi| = 0$ may be regarded (in Schmid's elegant depiction[1]) as droplets of condensate of radius ξ_{GL}, the Ginzburg-Landau (GL) coherence length. In the competing phase-disordering scenario, $|\Psi|$ remains finite above T_c. The collapse of the Meissner effect above T_c is caused instead by the vanishing of phase rigidity. Above T_c, fluctuations are primarily of the phase θ of Ψ, proceeding by phase slips caused by the motion of spontaneous vortices. In zero magnetic field, the net vorticity in the sample is zero, so the populations of "up" and "down" vortices are equal. In underdoped cuprates, there is strong evidence from Nernst,[2] magnetization,[3–5] and other experiments in support of the phase-disordering scenario.

Initially, it seemed to us that optimally doped $YBa_2Cu_3O_{7-y}$ (OPT YBCO), which has the largest interlayer coupling energy (and lowest electronic anisotropy) among the known cuprates, would be most amenable to standard mean-field (MF) treatment; i.e., its fluctuations above T_c are strictly Gaussian. Indeed, in the early 1990s, several groups applied the conventional Maki-Thompson Aslamazov-Larkin theory to analyze fluctuation conductivity above T_c.[6] Subsequently, these mean-field "fits," seemingly reasonable in OPT YBCO, were found to be woefully inadequate in underdoped YBCO and in most other cuprates. The steady accumulation of evidence from Nernst and torque experiments favoring the phase-disordering mechanism in underdoped hole-doped cuprates and in OPT $Bi_2Sr_2CaCu_2O_{8+y}$ (Bi 2212) has prompted a reassessment of the case for OPT YBCO. The recent torque magnetometry results in Ref. 5 have persuaded us that OPT YBCO is, in fact, much closer to the other hole-doped cuprates. The collapse of its Meissner state at T_c is also caused by vanishing of phase rigidity.

In a Comment, Rey *et al.*[7] have fitted the magnetization curves for OPT YBCO in Ref. 5 to their model and claimed that the diamagnetic signal is consistent with MF Gaussian fluctuations in a layered superconductor. Furthermore, they have extended their calculation to temperatures $T < T_c$ to infer an upper critical field H_{c2} that rises linearly with reduced temperature $(1 - T/T_c)$ with a slope of -3 T/K.

Here, we show that the fluctuation signal above T_c is just the tip of the iceberg. Because of strong interlayer coupling in OPT YBCO, it is necessary to go below T_c to uncover the close similarities with other cuprates. In Sec. II we describe the nonmonotonic variation of the magnetization curve just below T_c, previously noted in torque measurements on OPT Bi 2212.[4] This characteristic feature—inherent in the phase-disordering scenario—is common to the cuprates investigated to date. In Sec. III, we discuss the upper critical field H_{c2} for T close T_c in OPT YBCO. The striking inability of high-resolution experiments to detect the H_{c2} line, a cornerstone of the mean-field Gaussian picture, is also a characteristic feature of the phase-disordering mechanism. Finally, in Sec. IV we discuss the fits to the magnetization above T_c. We show that the conclusions of Rey *et al.*[7] are not valid.

II. NONMONOTONIC MAGNETIZATION

The curves of the diamagnetic component of the magnetization M_d in OPT YBCO (Ref. 5) are reproduced in Fig 1. At temperature T above ∼100 K, M_d is initially linear in H up to 6 T. As we approach T_c, the linear-response regime becomes confined to progressively smaller field ranges (for, e.g., $|H| < 2$ T at 95 K).

At $T_c = 92.5$ K (the present analysis shows that T_c is slightly higher than the nominal value in Ref. 5), the only significant change is a step increase in the magnitude $|M_d|$ near $H = 0^+$. Above 0.5 T, $M_d(H)$ is strikingly similar to the curves above T_c apart from vertical scale. We focus on the region in Fig. 1 bounded by the curves at T_c and 90 K (the curve at 91 K is representative). At $H = 0^+$, the step increase in $|M_d|$ signals the onset of full flux expulsion. However, a weak field interrupts this steep rise to produce a sharp cusp at the

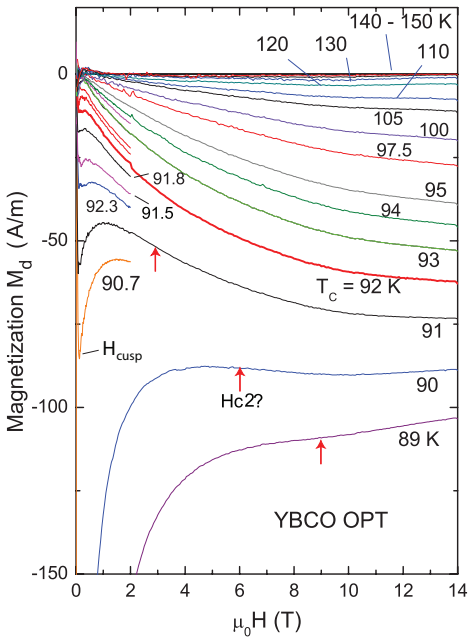

FIG. 1. (Color online) The field dependence of the diamagnetic component of the magnetization M_d in optimally doped $YBa_2Cu_3O_{7-y}$ at selected temperatures T. At $T_c = 92.5$, a weak step increase in $|M_d|$ signals the onset of full flux expulsion. Below T_c, a field $H > H_{cusp}$ causes a sharp decrease in the screening current, but at larger H, $|M_d|$ resumes its increase at a rate similar to that above T_c. This nonmonotonic pattern signals the field-induced decoupling of θ_n between adjacent bilayers below T_c. We argue that this is the defining magnetization feature that characterizes the transition in cuprates. μ_0 is the vacuum permeability. The arrows (labeled as H_{c2}?) are H_{c2} values at 89, 90, and 91 K predicted in Ref. 7. (Adapted from Ref. 5.)

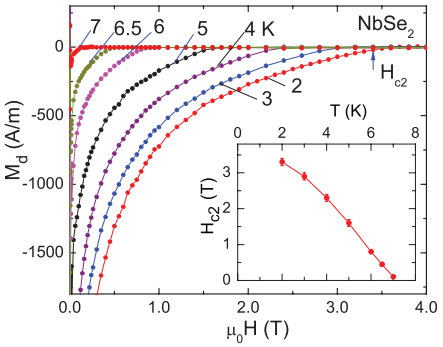

FIG. 2. (Color online) The magnetization curves below T_c in $NbSe_2$. At each T, $M_d(H)$ decreases monotonically to reach zero at $H_{c2}(T)$. Following vortex entry at H_{c1} (not resolved here), the diamagnetic screening currents are steadily weakened as H suppresses the pair amplitude. The inset plots the inferred H_{c2} vs T. (Adapted from Ref. 3.)

field H_{cusp} (H_{cusp} is slightly higher than the lower critical field H_{c1} because of surface pinning of vortices). When H exceeds H_{cusp}, $|M_d|$ falls rapidly to a broad minimum near 1 T, but subsequently *rises* to even larger values. This nonmonotonic profile in M_d, appearing just below T_c, is a defining hallmark of the transition in cuprates. In this interval (90–92.5 K), M_d vs H is reversible except in the vicinity of H_{cusp}, where surface-barrier pinning of vortices causes a slight hysteresis.

This unusual nonmonotonic profile—absent in low-T_c superconductors to our knowledge—implies the following picture. The collapse of the Meissner state at H_{cusp} leads to a steep decrease in $|M_d|$ as vortices enter the sample. This is a consequence of field suppression of the nascent inter-bilayer phase coupling. (The two CuO_2 layers bracketing the Y ions constitute a bilayer. We are concerned with only the coupling between adjacent bilayers which are separated by a spacing $d = 11.8$ Å. We mention the intra-bilayer coupling below.) In low-T_c superconductors, the decrease invariably continues monotonically to zero as $H \to H_{c2}(T)$ (the upper critical field at temperature T). For reference, we show in Fig. 2 curves of M_d vs H in the layered superconductor $NbSe_2$.[3] By contrast, the nonmonotonicity in $|M_d|$ implies that the diamagnetic current in OPT YBCO turns around and grows *stronger* with H at a rate closely similar to that above T_c. Remarkably, if we hide the field region around H_{cusp}, the profiles of M_d vs H below T_c resemble those above T_c, apart from a different vertical scale. This implies that the transition at T_c at which flux expulsion appears is a weak-field phenomenon. Beyond this weak-field regime, there is no hint that a transition has occurred.

Returning to Fig. 1, we interpret the unusual nonmonotonic pattern (now seen in Bi 2201, Bi 2212, LSCO and YBCO)[3–5] as reflecting the rapid growth of c-axis phase rigidity below T_c (in zero or weak H) and its subsequent destruction at H_{cusp}. In a finite interval above T_c, the pair wave function $|\Psi_n|e^{i\theta_n}$ in bilayer n has a finite average amplitude $\langle|\Psi_n|\rangle$. The in-plane phase-phase correlation length ζ_a in each bilayer, given by

$$\langle e^{-i\theta_n(0)} e^{i\theta_n(\mathbf{r})}\rangle = e^{-r/\zeta_a}, \qquad (1)$$

is long enough that local diamagnetic currents can be detected by torque magnetometry. However, the c-axis correlation length $\zeta_c \ll d$, so θ_n is uncorrelated between adjacent bilayers. Hence M_d reflects the diamagnetic response of 2D supercurrents which are observable to very intense H. In Fig. 1, this 2D diamagnetic response is represented in the field profile of M_d at 94 K.

Below T_c, ζ_c diverges (in zero H) to lock θ_n across all bilayers. In weak H, the 3D phase rigidity produces full expulsion. However, in the 2-K interval 90–92.5 K, a weak field $H \sim H_{cusp}$ suffices to destroy the c-axis phase stiffness. The system then reverts back to the diamagnetic response of 2D uncorrelated condensates. Consequently, as H increases further, the 2D diamagnetic response continues to increase, mimicking the profile at 94 K. At 14 T, the 2D response leads to a value for $|M_d|$ that well exceeds its value at H_{cusp} (see 91-K curve). The weak locking of θ_n across bilayers and the field-induced unlocking account for the nonmonotonicity of M_d as well as the similarities of the high-field portions across T_c in a physically reasonable way. The juxtaposition of an extremely large pairing energy scale (d-wave gap amplitude $\Delta \sim 40$ mV) and a weak c-axis phase stiffness leads to this very unusual phase locking-unlocking scenario which seems pervasive in the hole-doped cuprates. We argue that this situation cannot be treated by applying the mean-field GL approach[1] to the Lawrence-Doniach (LD) Hamiltonian.[8,9]

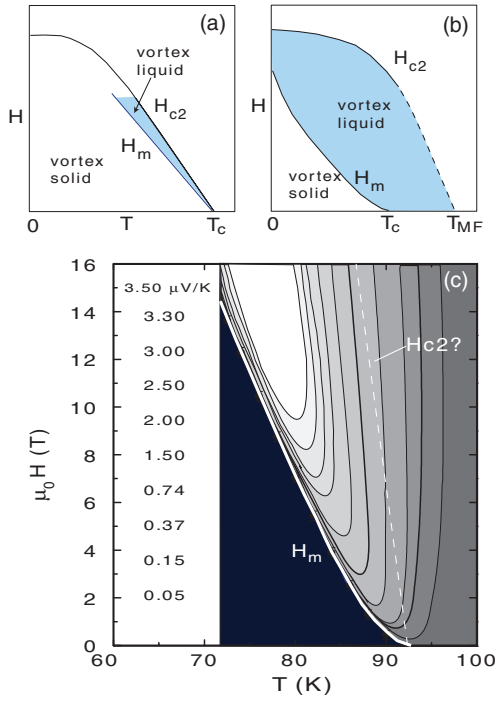

FIG. 3. (Color online) Profiles of the melting field $H_m(T)$ and upper critical field $H_{c2}(T)$ in low-T_c and cuprate superconductors. Panel (a) shows the phase diagram for a conventional type-II superconductor in the T-H plane. The vortex liquid phase is wedged between the curves of $H_m(T)$ and $H_{c2}(T)$, both of which terminate at T_c as $H \to 0$. In the hole-doped cuprates [panel (b)], the vortex liquid state dominates the phase diagram. As $H \to 0$, $H_m(T)$ terminates at the observed T_c whereas $H_{c2}(T)$ terminates at a higher temperature T_{MF}. Panel (c): The contour plots of the magnitude of the Nernst signal e_y in OPT YBCO in the T-H plane. Values of the 10 contours are displayed on the left column. The melting field $H_m(T)$ separates the vortex solid (black region) from the vortex liquid state. The dashed line is the H_{c2} line predicted in Ref. 7. (Adapted from Ref. 11.)

III. CLOSURE OF THE H_{c2} CURVE

Another strong argument against the mean-field description is obtained from the qualitative features of the phase diagram in the T-H plane (Fig. 3). A cornerstone of the mean-field Gaussian description of a type-II superconductor is the well-known profile of the upper critical field curve $H_{c2}(T)$ [Fig. 3(a)]. In the T-H plane, the H_{c2} curve is a sharply defined boundary that separates the region with finite pair amplitude $|\Psi|$ from the normal state with $|\Psi| = 0$. The Gaussian fluctuations are fluctuations of the amplitude around the $|\Psi| = 0$ state above $H_{c2}(T)$. In low-T_c superconductors (for $T \gtrsim 0.5\,T_c$), $H_{c2}(T)$ decreases linearly in the reduced temperature $t = 1 - T/T_c$ to terminate at T_c. This profile is shown for $NbSe_2$ in the inset of Fig. 2. To stress this point, we refer to the termination as "closure" of the curve of H_{c2}.

The closure of H_{c2} reflects an anomalous aspect of the BCS transition at T_c. As T is elevated above T_c in zero H, the pair condensate vanishes before it loses its phase rigidity. This implies that both the superfluidity (which depends on finite phase rigidity) and the physical entities that manifest long-range phase coherence (the Cooper pairs) vanish at the same temperature T_c. (This is akin to having the local moments in an antiferromagnet vanish at the Néel temperature.) In an applied field H, phase rigidity is maintained if the vortices are in the solid state (and pinned). As H approaches H_{c2}, the phase rigidity abruptly vanishes at the melting field H_m which marks the transition to the vortex-liquid state (the analog of the paramagnetic state in the antiferromagnet). The vortex-liquid state is wedged between the curves of $H_m(T)$ and $H_{c2}(T)$ [Fig. 3(a)]. As sketched, the anomalous feature in the BCS scenario is that, as $H \to 0$, the vortex-liquid region vanishes.

The competing phase-disordering scenario has a qualitatively different phase diagram [Fig. 3(b)]. The vortex liquid state now occupies a much larger fraction of the region in which $|\Psi| \neq 0$. Significantly, the melting curve $H_m(T)$ intercepts the $H = 0$ axis at a temperature $T_m(0)$ lower than the termination point T_{MF} of the H_{c2} curve, as sketched in panel (b). If we increase T along the $H = 0$ axis, phase rigidity is lost at $T_m(0)$ long before we reach T_{MF}. Since both the Meissner effect and the zero-resistivity state are crucially dependent on having long-range phase stiffness, the T_c commonly observed by these techniques is identified with $T_m(0)$.

Above T_c, we have a vortex liquid whose existence may be detected using the Nernst effect and torque magnetometry (resistivity is ineffectual). The onset temperatures T_{onset} for the vortex Nernst and diamagnetic signals[2,5] are lower bounds for T_{MF}. Clearly, if the interval $[T_c, T_{MF}]$ is large (underdoped cuprates), the curve of $H_{c2}(T)$ is nearly T independent in the interval $0 > T > T_c$; it attains closure only at T_{MF}. [The T-independent part has been established in underdoped, single-layer Bi 2201 where H_{c2} ($\sim$50 T) is nearly accessible with a 45-T magnet.[5]] Hence, if we focus on experiments close to T_c, the only curve that intersects the $H = 0$ axis is the melting curve. Even at T_c, H_{c2} is inaccessible except for Bi 2201. The absence of closure for $H_{c2}(T)$ implies that the vortex-liquid state extends above T_c to T_{MF}, and survives to $H \sim H_{c2}$.

A striking empirical fact in the hole-doped cuprates is that experiments (over a 25-year period) have never observed an H_{c2} curve that decreases linearly with t to terminate at T_c (not counting early flux-flow resistivity experiments that misidentified H_m for H_{c2}). The absence of the H_{c2} curve is incompatible with the Gaussian picture, but anticipated in the phase-disordering scenario.

We now turn to results in OPT YBCO. Figure 3(c) displays the contour plots of the Nernst signal e_y in another OPT YBCO crystal with identical T_c and closely comparable quality (adapted from Ref. 11). The Nernst signal is defined as $e_y = E_y/|\nabla T|$, where E_y is the transverse electric field produced by the velocity of vortices diffusing in the applied thermal gradient $-\nabla T$ (see Ref. 2). In the vortex solid [$H < H_m(T)$], e_y is rigorously zero. Just above $H_m(T)$, e_y rises very steeply reflecting the steep increase in vortex velocity in the liquid state. In comparison with similar contour plots for underdoped cuprates (as well as OPT Bi 2212), the interval $[T_c, T_{MF}]$ in OPT YBCO is smaller. Also, the curve $H_m(T)$ rises from T_c with a much steeper slope. Nevertheless, the contour features are qualitatively similar. The contours are very nearly vertical at T_c, implying that e_y hardly changes with H. Even exactly at T_c, there is no field scale above which the system can be described as being in the "normal state" with $|\Psi| = 0$. In cuprates, we find it helpful to regard the segment of the $H = 0$ axis between T_c and T_{MF} as the continuation of the $H_m(T)$

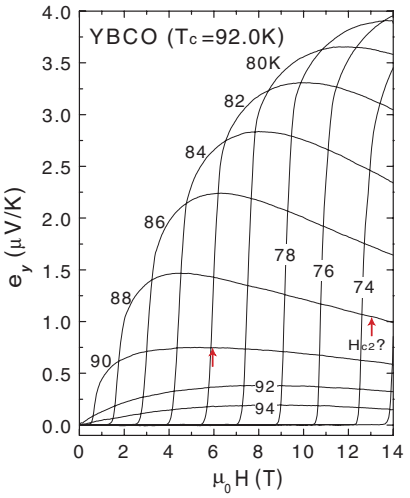

FIG. 4. (Color online) Plots of the Nernst signal $e_y = E_y/|\nabla T|$ vs H in OPT YBCO with $T_c = 92$ K at selected T (E_y is the Nernst E field and $-\nabla T$ the applied temperature gradient). At the melting field H_m, e_y rises nearly vertically reflecting the sharp increase in vortex velocity. The contour map [Fig. 3(c)] was derived from these curves (and additional curves not plotted). The "up" arrows denote the values for H_{c2} at 88 and 90 K predicted in Ref. 7. (Adapted from Ref. 10.)

curve. The vortex liquid, confined between the curves of H_m and H_{c2} below T_c, expands to occupy the entire region below H_{c2} above T_c. It plays a dominant role in thermodynamic measurements.

In Ref. 7, the H_{c2} line is predicted to increase linearly with t from the point $(T = T_c, H = 0)$ with a slope of -3 T/K. We have drawn their H_{c2} line as a dashed line (labeled as $Hc2$?) in Fig. 3(c). Clearly, the predicted H_{c2} line cuts across the contours in an arbitrary way that bears no resemblance to experiment.

To explain this better, we show in Fig. 4 the profiles of e_y vs H at selected fixed T near T_c.[10] Just below T_c (curves at 90 and 88 K), e_y rises nearly vertically when H exceeds H_m, reflecting the sharp increase in the vortex velocity in the vortex liquid in response to the gradient $-\nabla T$. The magnitude of e_y, which remains large up to 14 T, implies that $|\Psi|$ remains finite. There is no experimental feature (change in slope, for example) that signals $|\Psi| \to 0$ at the values of H_{c2} predicted by Rey *et al.* (shown as "up" arrows).

The same difficulty exists for the plots of M_d vs H in Fig. 1, where the predicted H_{c2} values are indicated by the arrows. Contrary to the claim in Ref. 7, the curves of M_d vary smoothly through the predicted field values at 89, 90, and 91 K. Again, there is no feature reflecting either a transition or crossover. Given that $|M_d|$ is a measure of the supercurrent density J_s surrounding each vortex in the sample (even in the vortex liquid state), we would expect $|M_d|$ to be considerably larger when $|\Psi|$ is finite ($H < H_{c2}$) compared with the Gaussian fluctuation regime above H_{c2}. Instead, $|M_d|$ hardly varies as H crosses the predicted values. One confronts the very awkward problem of explaining why $|M_d|$ retains nearly the same value below and above "H_{c2}." Even worse, close to T_c (curve 91 K), $|M_d|$ actually increases when H exceeds 3 T (this reflects the decoupling of the bilayers as discussed in Sec. II).

IV. FLUCTUATIONS ABOVE T_c

We comment on the fits above T_c reported in Ref. 7. Figure 5 shows plots of the susceptibility $\chi = M/H$. Above 100 K, χ is H independent over a large field region. However, as T falls below 100 K, the linear response is confined to progressively smaller field ranges, as mentioned. Nonetheless, as $T \to T_c^+$, the linear-response value of χ (dashed lines in Fig. 5) does not diverge. Instead, the appearance of the Meissner effect (and its subsequent suppression by H) occur at much lower field scales as discussed. Below T_c, the hallmark nonmonotonicity of M_d vs H described above is harder to see in plots of χ vs H because of the strong field variation caused by dividing a relatively flat profile by H.

Moving to the fluctuation regime above T_c, we show in Fig. 6 the plots of χ vs T at selected values of H. Above T_c, all values of χ below 2 T collapse to a single curve, which defines the linear-response fluctuation susceptibility that can be directly compared with mean-field theories.[1,8,9] For illustration, we show as a dashed curve the best fit to the linear-response MF expression[8]

$$\chi(T) = -\frac{\eta}{\sqrt{[\epsilon^2 + \epsilon B_{LD}]}}, \tag{2}$$

with η an adjustable numerical factor and $\epsilon = (T - T_c)/T_c$ (the dashed curve has $\eta = 3.78 \times 10^{-7}$). For the LD parameter, we used the value proposed by Rey *et al.*[7] ($B_{LD} = 0.11$).

While the fit can account for the overall magnitude of χ above 100 K with reasonable parameters, as shown by Rey *et al.*, the functional form in Eq. (2) does not describe the data trend all that well. Between 94 and 98 K, it underestimates $|\chi|$ by as much as 15%, and overestimates its value at 92.5 K. A similar pattern of overshooting and undershooting is also evident in Fig. 1(a) of Rey *et al.*

At large H (curves at 6 and 14 T), χ varies smoothly through T_c without detectable change in slope. This reflects the

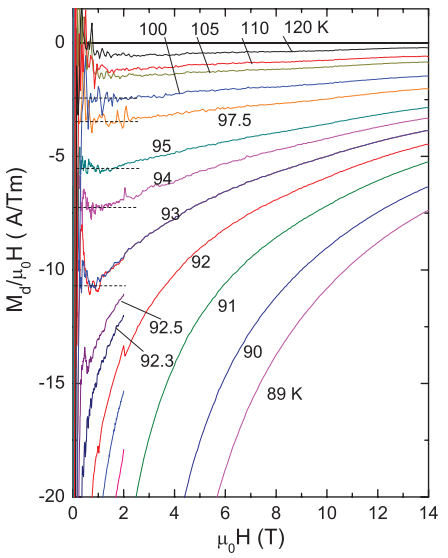

FIG. 5. (Color online) Plots of the susceptibility $\chi = M/H$ vs $\mu_0 H$ in OPT YBCO at selected T ($T_c = 92.5$ K). The dashed horizontal lines indicate the linear-response region for curves near T_c.

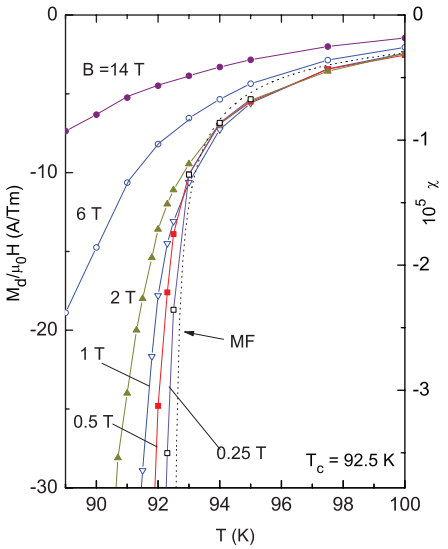

FIG. 6. (Color online) The T dependence of the susceptibility in OPT YBCO for selected values of H. Above T_c (92.5 K), χ is H independent below 2 T (linear response region). Below T_c, χ becomes strongly H dependent at low H because of the field suppression of phase locking in the vicinity of $H_{\rm cusp}$. At large H (curves at 6 and 14 T), χ varies smoothly through T_c. The dashed line is the mean-field (MF) fit to Eq. (2) with $\eta = 3.78 \times 10^{-7}$ and $B_{LD} = 0.11$.

continuity of the diamagnetic response in strong fields described above. Significantly, at low H, the linear-response segment of χ suddenly becomes strongly H dependent even in very weak H. As we discussed, this reflects the nonmonotonicity that appears above the field $H_{\rm cusp}$. These features cannot be described by the Gaussian approach of Rey *et al.*[7]

V. SUMMARY

In attempting to understand the fluctuation signals of the magnetization in OPT YBCO, it is essential to view the results above and below T_c. We show that the nonmonotonic curves of M_d vs H just below T_c are consistent with the loss of long-range phase coherence in a layered superconductor with extremely large pair-binding energy within each layer, but a c-axis coupling (between bilayers) that is suppressed by a few teslas close to T_c. These features are incompatible with the Gaussian picture. In addition, when discussing the thermodynamics of hole-doped cuprates, we argue that it is vital to recognize the elephant in the room, namely the vortex liquid above and below T_c. The dominant presence of the vortex liquid alters qualitatively the profiles of the H_{c2} curve, pushing its closure to a temperature higher than T_c. As a result, the cornerstone feature of the Gaussian approach, namely an H_{c2} line that terminates at T_c, is absent in OPT YBCO (and other hole-doped cuprates). This contradicts a prediction of Ref. 7.

In the phase-disordering picture, the d-wave pairing gap Δ must persist high above T_c. Spectroscopic experiments are increasingly able to distinguish between the gap in the vicinity of the node from the much larger antinodal gap. The persistence of the nodal Δ above T_c has now been reported in scanning tunneling microscopy[12] and photoemission experiments[13,14] on OPT Bi 2212, and in c-axis infrared reflectivity experiments on YBCO.[15] The vanishing of the Meissner effect above T_c reflects the collapse of the interbilayer phase coupling. Since the intra-bilayer phase coupling is much stronger, one might expect that the concomitant phase rigidity can be observed experimentally above T_c. Recently, this was detected by Dubroka *et al.*[16] as a Josephson plasma resonance that persists above T_c over a broad doping range in YBCO (as high as 180 K in the underdoped regime). For a recent susceptibility experiment in LaSrCuO directly relevant to nonlinear magnetization (Sec. II), see Ref. 17.

ACKNOWLEDGMENTS

We have benefited from valuable discussions with Zlatko Tesanovic, Oskar Vafek, Steve Kivelson, Ashvin Vishwanath, Sri Raghu, Ali Yazdani, Christian Bernhard, and P. W. Anderson. Support from the U.S. National Science Foundation under MRSEC Grant No. DMR 0819860 is gratefully acknowledged.

[1] Albert Schmid, Phys. Rev. **180**, 527 (1969).
[2] Yayu Wang, Lu Li, and N. P. Ong, Phys. Rev. B **73**, 024510 (2006).
[3] Yayu Wang, Lu Li, M. J. Naughton, G. D. Gu, S. Uchida, and N. P. Ong, Phys. Rev. Lett. **95**, 247002 (2005).
[4] Lu Li, Yayu Wang, M. J. Naughton, S. Ono, Yoichi Ando, and N. P. Ong, Europhys. Lett. **72**, 451 (2005).
[5] Lu Li, Yayu Wang, Seiki Komiya, Shimpei Ono, Yoichi Ando, G. D. Gu, and N. P. Ong, Phys. Rev. B **81**, 054510 (2010).
[6] For an especially detailed investigation, see Kouichi Semba, Takao Ishii, and Azusa Matsuda, Phys. Rev. Lett. **67**, 769 (1991).
[7] R. I. Rey, A. Ramos-Alvarez, J. Mosqueira, M. V. Ramallo, and F. Vidal, Phys. Rev. B **87**, 056501 (2013).
[8] K. Yamaji, Phys. Lett. A **38**, 43 (1972).
[9] M. V. Ramallo, C. Torrón, and Félix Vidal, Physica C **230**, 97 (1994).
[10] N. P. Ong, Yayu Wang, S. Ono, Yoichi Ando, and S. Uchida, Ann. Phys. (Leipzig) **13**, 9 (2004).
[11] Yayu Wang, N. P. Ong, Z. A. Xu, T. Kakeshita, S. Uchida, D. A. Bonn, R. Liang, and W. N. Hardy, Phys. Rev. Lett. **88**, 257003 (2002).
[12] Kenjiro K. Gomes, Abhay N. Pasupathy, Aakash Pushp, Shimpei Ono, Yoichi Ando, and Ali Yazdani, Nature (London) **447**, 569 (2007).
[13] T. J. Reber and D. S. Dessau, reported at American Physical Society March Meeting, 2012.
[14] Takeshi Kondo, Yoichiro Hamaya, Ari D. Palczewski, Tsunehiro Takeuchi, J. S. Wen, Z. J. Xu, Genda Gu, Jörg Schmalian, and Adam Kaminski, Nat. Phys. **7**, 21 (2011).
[15] N. Murai, T. Masui, M. Ishikado, S. Ishida, H. Eisaki, S. Uchida, and S. Tajima, Phys. Rev. B **85**, 020507(R) (2012).
[16] A. Dubroka, M. Rössle, K. W. Kim, V. K. Malik, D. Munzar, D. N. Basov, A. A. Schafgans, S. J. Moon, C. T. Lin, D. Haug, V. Hinkov, B. Keimer, Th. Wolf, J. G. Storey, J. L. Tallon, and C. Bernhard, Phys. Rev. Lett. **106**, 047006 (2011).
[17] G. Drachuck, M. Shay, G. Bazalitsky, J. Berger, and A. Keren, Phys. Rev. B **85**, 184518 (2012).